Identification of Failure Modes for Circuit Samples with Confounded Causes of Failure

Shu-han Hsu, Ying-Yuan Huang, Kexin Yang, and Linda Milor School of Electrical and Computer Engineering Georgia Institute of Technology Atlanta, GA 30332, USA

Abstract—Circuits may fail in the field due to a wide variety of failure modes. If there are frequent failures in the field, circuits are returned to the manufacturer, and the causes of failure must be identified. The challenge is that wearout mechanisms are confounded in circuit and system-level failure data. Using such failure data, it is often hard to separate the underlying failure causes without time-consuming and expensive physical failure analysis. To distinguish the wearout mechanisms for each failure sample, we have developed a quick and low-cost methodology using maximum likelihood estimation and probability analysis to determine the origin of the failure distributions, region of error, and sorting accuracy. We apply our methodology to analyze the competing wearout mechanisms in 14nm FinFET ring oscillators, as an example, using simulation. We also consider the problem of Trojan detection.

Keywords—Time-dependent dielectric breakdown (TDDB); Electromigration (EM); Weibull distribution; Lifetime; Wearout; FinFET; Trojan

I. INTRODUCTION

The increasing complexity of today's integrated circuits creates a need to diagnose the causes of wearout failures, especially when failure rates are different than expected. The need to diagnose the causes of failure in the field is also increasing with the outsourcing of fabrication, which leads to vulnerabilities to malicious attacks with hardware trojans utilizing wearout mechanisms to damage chips, causing major concerns for defense systems [1]-[3]. For circuits and systems, wearout mechanisms are often confounded, making it difficult to identify the root cause for breakdown in each sample without physical failure analysis, which is time-consuming, damages the sample, and costly [4], [5]. In this paper, we develop a methodology to identify the probabilistic origin of failure for each monitored sample, determine the region of error indicating the time period where the cause of failure is unknown, and analyze the sorting accuracy. In doing so, we select better samples for physical failure analysis, saving time and money. Specifically, we use machine learning to identify samples that are likely to fail due to each wearout mechanism and those samples whose cause of failure is unknown. This second group of samples should be prioritized for physical failure analysis.

Generally, wearout models are developed using test structures, which are designed to isolate failure modes. These test structures may not be reflective of the actual system-level design. In circuits, there is a risk of interactions that may cause circuits to fail in ways not predicted by the models. This study uses 14nm FinFET ring oscillators as a circuit vehicle to extract wearout data, focusing on the front-end vs. back-end mechanisms. Ring oscillators have behaviors similar to circuits.

Like circuits, they have confounded wearout data similar to system-level failure data. The various ring oscillators are based on the 14nm FinFET pdk technology node design kit jointly developed by IBM, GlobalFoundries (GF), and Samsung.

This work is a simulation study to test our methodology. We use lifetime simulation of circuits to generate the data sets [6]-[8], with lifetime simulation models calibrated to test structure data. We account for stress of layout geometries and transistors, based on circuit operating conditions.

In our methodology, we first apply maximum likelihood analysis and the Weibull distribution to failure data to detect the overall set of Weibull parameters for the first and secondary wearout mechanisms. Then, with the known competing Weibull parameters, we apply the probability distribution of each mechanism at each failure time to assign the most likely and dominant wearout mechanism for each sample. Next, we demonstrate how to find the region of error (time interval when the uncertainty is highest), and the accuracy of the assignment for each sample. The contributions are (a) a mathematical approach to find the parameters of wearout distributions from data where the failure rate distributions come from more than one wearout mechanism, (b) the identification of the probabilistic cause of each sample, to guide the selection of samples for physical failure analysis, and (c) the identification of time points with the greatest uncertainty in the cause of failure for the samples.

This paper is organized as follows. Section 2 provides background information on the wearout models used in this study and the generation of dataset with more than one wearout mechanism. Section 3 provides the theory on how to calculate Weibull parameters from the data and the probabilistic cause of each sample. We then analyze our ring oscillators in Section 4 with the above methodology described in detail in Section 3. In Section 5 we consider the application of Trojan detection. The paper concludes in Section 6 with a summary.

II. WEAROUT MODES

A. Wearout Models

The investigation of front-end vs back-end breakdown mechanisms is explored in this study, using front-end of line time-dependent dielectric breakdown (FEOL TDDB, GTDDB) and electromigration (EM). FEOL TDDB is one of the most common front-end breakdown mechanisms, while EM is one of the leading causes of backend failures. GTDDB occurs due to the build-up of traps in the gate oxide region. EM is the dislocation of atoms in interconnect metals from the momentum transfer of atoms. The wearout models for these two

TABLE I WEAROUT MODELS [9]-[11]

Mechanism	Model
GTDDB	$\eta = A_{FEOL}(WL)^{\frac{-1}{\beta}}e^{\frac{-1}{\beta}}V^{a+bT}exp\left(\frac{cT+d}{T^2}\right)s^{-1}$ where a, b, c, d , and A_{FEOL} are process-dependent constants. V and T are voltage and temperature. W and L are the width and length of the MOSFET device.
EM	$\eta = A_{EM}J^{-n}\exp(E_A/kT)$ where A_{EM} is a constant, T is temperature, J is current density, E_a is the activation energy (0.85 eV), n=1 (void growth), and k is Boltzmann constant.

mechanisms are summarized in Table I [9]-[11].

These breakdown mechanisms can be described using the Weibull distribution with two parameters, η and β . η is the characteristic lifetime, which is the time-to-failure of a sample at 63% failure probability, and β is the shape parameter that describes the spread of the distribution of failure samples. The parameters used were obtained from experimental data [11]-[15].

B. Competing Wearout Mechanisms

The confounded failure data in circuits are composed of competing wearout mechanisms, which occur when failures are due to more than one breakdown mechanism, independent of each other (mechanisms do not affect each other). For a failure sample that has two wearout mechanisms, mechanism 1 and mechanism 2, the competing failure probability density function of the overall system, f(t), can be described below [16]:

$$f(t) = f_1(t) * R_2(t) + f_2(t) * R_1(t)$$
 (1) where $f_1(t)$ is the probability density function and $R_1=1-F_1(t)$ is the survival function for mechanism 1, respectively. $F_1(t)$ is the cumulative distribution function for mechanism 1. $f_2(t)$ is the probability density function and $R_2=1-F_2(t)$ is the survival function for mechanism 2, respectively. Usually one of these mechanisms will be the dominant failure mechanism, which is determined by both the β and η values, and the other mechanism will be the secondary mechanism.

The competing probability density function contribution from mechanism 1, called a₁, is defined below:

$$a_1 = f_1(t) * R_2(t)$$
 (2)

which is the probability density function portion of the overall system showing that mechanism 1 has failed but mechanism 2 is still working. Similarly, the competing probability density function contribution from mechanism 2, called a₂, is defined below:

$$a_2 = f_2(t) * R_1(t)$$
 (3)

When the differences in the individual probability density functions are large, the failure mechanism that fails much later will have a survival function close to 1, and the other mechanism that fails first will have a survival function close to 0. This will simplify the competing probability density function contribution to the dominant probability density function.

The competing failure probability density function is different than the mixed Weibull probability density function [17]:

$$f(t) = a * f_1(t) + b * f_2(t)$$
 (4)

where a and b are the mixed weights. The mixed Weibull probability density function occurs when the breakdown is due to both mechanisms at the same time.

For the competing Weibull probability density function, the breakdown at a specific failure time is due to only one mechanism, but the cause can be from either mechanism 1 or 2, but not both. The wearout mechanisms are independent and each wearout mechanism has no influence on failures due to the other mechanism. This is reasonable for GTDDB and EM, since they impact different components of the circuit (the transistor and the backend interconnect, respectively).

III. METHODOLOGY FOR IDENTIFYING COMPETING WEAROUT MECHANIMS FOR EACH SAMPLE

A. Extraction of Weibull Parameters

In order to investigate the competing failure mechanisms, the Weibull parameters for each set of competing mechanisms of various 501-stage ring oscillators are shown in Table II. The ratio of the β values for the two competing failure mechanisms were varied to explore the effect of the shape parameter's influence in detecting the correct failure distribution for each sample. All other parameters were kept the same. In all studies, GTDDB and EM are mechanism 1 and mechanism 2, respectively.

The failure distribution of the competing mechanisms is modeled by picking a point randomly from each distribution. Then, the smaller value is set as the lifetime, because it is the mechanism that fails first at that time point. Next, the points are plotted as ordered pairs: $(\ln(t_1), \ln(-\ln(1-(\frac{1}{2N}))), (\ln(t_2), \ln(-\ln(1-(\frac{3}{2N}))))$, etc. Sample sizes N of 10, 100, and 1000 were generated for each set to investigate the effect of sample size, which are shown in Fig. 1.

B. Maximum Likilhood Estimation

As a preliminary analysis step, maximum likelihood estimation (MLE) is used to determine the overall parameters present in the competing wearout modes, but it does not assign the individual samples to their corresponding failure distributions. From the given observations, which are the failure times in our examples, MLE finds the parameter values that maximize the likelihood or highest probability of getting the observations given the parameters. The likelihood function for uncensored data is [16]:

$$\mathcal{L}(\theta) = C \prod_{i=1}^{N} f(t_i)$$
 (5)

where θ is the set of competing Weibull parameters, β_1 , η_1 , β_2 , η_2 . The log likelihood function can be written as: $\ln \mathcal{L}(\theta) = \sum_{i=1}^N \ln f(t_i) + \ln C$

$$ln \mathcal{L}(\theta) = \sum_{i=1}^{N} ln f(t_i) + ln \mathcal{C}$$
(6)

TABLE II COMPETING WEIBULL PARAMETERS [11]-[15]

Set	β1	η ₁ (yrs)	$\begin{array}{c ccccccccccccccccccccccccccccccccccc$		β ratio for 1st vs 2nd mechanism
1	10	9.87	1.14	25.1296	8.77
2	5	9.87	1.14	25.1296	4.39
3	1.64	9.87	1.14	25.1296	1.44

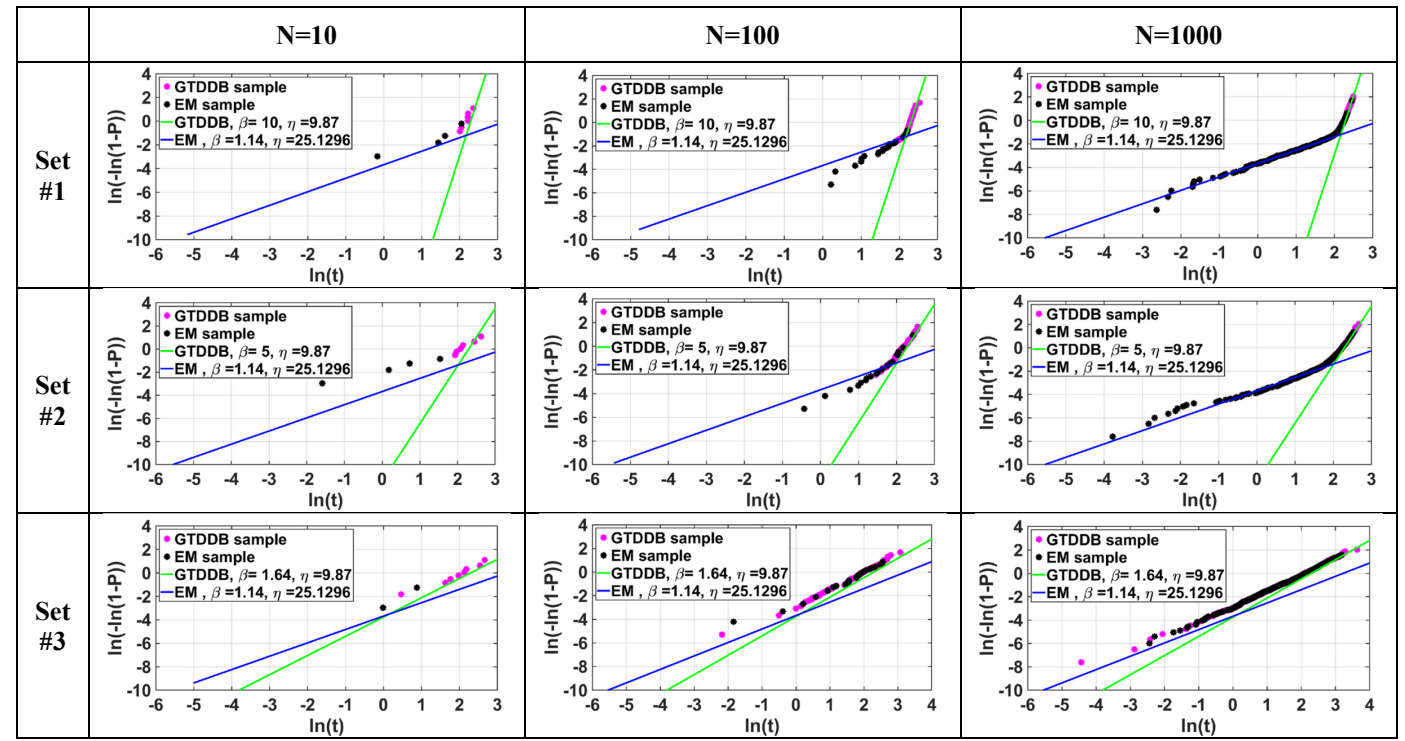


Fig. 1. Failure distribution for case studies with varying sample sizes from 10 to 1000 samples (unit of time: yrs). P is probability. Pink markers are samples from 1st wearout mechanism, while the black markers are samples from 2nd wearout mechanism.

Various methods can be used to solve eq. (6), and we chose to use the quasi-Newton method [18], which is a type of machine learning algorithm, due to its simple implementation. For sample sizes of 10, the initial conditions for both the β and η were varied at the same time in increments of 5% from -5% to 5%, and the average of each parameter was taken over all mechanisms. The range of -5% to 5% was chosen, because the MLE was usually unable to separate the competing Weibull parameters beyond this range. Similarly, for sample sizes of 100 and 1000, the initial conditions for both β and η were varied at the same time in increments of 5% from -15% to 15%, and the average of each parameter was taken over all increments as the set of overall parameters for the competing mechanisms. For

these two cases, the range of -15% to 15% was chosen, because the MLE also was usually unable to separate the competing Weibull parameters beyond this range.

The results for the MLE extracted Weibull parameters for all sets are summarized in Table III, along with the average of the absolute error over all deviations for the extracted parameters. As an overall trend, generally the absolute error increases with decreasing β ratio and sample size. Occasionally, there may be some sets that have a larger absolute MLE error, because the MLE may be stuck in a local minimum, but this error is still less than 45%. In fact, most of the absolute errors are still in a reasonable range, which is less than 30%. These errors can be

TABLE III
AVERAGED MLE EXRACTED WEIBULL PARAMETERS FOR ALL SETS

	Sample Size		GTI	ODB		EM				
		β average	β absolute error average	η average	η absolute error average	β average	β absolute error average	η average	η absolute error average	
	10	8.604	13.963%	9.260	6.176%	1.113	3.336%	17.831	29.044%	
Set #1	100	10.894	8.942%	10.112	2.453%	1.632	43.155%	20.357	18.992%	
π1	1000	10.269	2.687%	9.899	0.291%	1.154	1.195%	24.286	3.358%	
~ .	10	3.700	25.998%	10.678	8.185%	0.736	35.442%	15.745	37.344%	
Set #2	100	4.874	2.520%	9.580	2.934%	1.452	27.378%	23.203	13.062%	
	1000	5.201	4.017%	9.927	0.576%	1.079	5.311%	30.080	19.699%	
	10	2.087	27.273%	9.667	2.057%	0.924	18.986%	24.973	4.671%	
Set #3	100	1.917	16.917%	9.267	6.108%	0.996	12.598%	23.042	8.771%	
	1000	1.708	4.169%	11.032	11.778%	1.069	6.200%	20.539	20.286%	

minimized further by optimizing the calculation procedure for performing MLE.

C. Sorting of Weibull Parameters for Each Sample

With the overall Weibull parameters for each set now known, each failure sample can be sorted into its respective failure distribution. For each failure time point, the time-tofailure value can be inputted into each competing probability density function contribution, eq. (2) and eq. (3), for each distribution. A higher value represents the higher probability of the sample belonging to that respective distribution. Therefore, we are comparing the relative values, or ratio of eq. (2) to eq. (3), to sort the samples.

An interesting phenomenon is that for the case of competing wearout mechanisms, the relative values or the ratio of the hazard function is also the same as comparing eq. (2) to eq. (3). The hazard function for mechanism 1 is:

$$h_1(t) = \frac{f_1(t)}{R_1(t)} \tag{7}$$
 and similarly, the hazard function for mechanism 2 is:
$$h_2(t) = \frac{f_2(t)}{R_2(t)} \tag{8}$$

$$h_2(t) = \frac{f_2(t)}{R_2(t)} \tag{8}$$

The hazard function, also known as the instantaneous failure rate, shows the conditional probability of a failure given that the system is currently working. When multiplying both sides of eq. (7) or eq. (8) by $R_1(t) * R_2(t)$, they can be rewritten as:

$$R_1(t) * R_2(t) * h_1(t) = f_1(t) * R_2(t)$$
 (8)

and:

$$R_1(t) * R_2(t) * h_2(t) = f_2(t) * R_1(t)$$
 (9)

where the right sides of eqs. (8) and (9) equal eqs. (2) and (3), respectively. Since only the relative values or ratio, not the absolute value, is needed, using the hazard function to sort the samples has the same results as using the competing probability density function contributions.

D. Calculations for Region of Error and Accuracy of Sorting

Looking back at eq. (1), at any time point, the competing failure probability is always composed of two contributions, $f_1(t)$ * $R_2(t)$ and $f_2(t)$ * $R_1(t)$. As mentioned previously, $f_1(t)$ * $R_2(t)$ is the contribution from mechanism 1, where mechanism 1 has failed but mechanism 2 has not failed, and $f_2(t) * R_1(t)$ is the contribution from mechanism 2, where mechanism 2 has failed but mechanism 1 has not failed. Therefore, x, which is the percentage of failures from mechanism 1 at a given time t, is:

$$\chi = \frac{f_1(t) * R_2(t)}{f_1(t) * R_2(t) + f_2(t) * R_1(t)}$$
(10)

and y, which is the percentage of failures from mechanism 2 at a given time t, is:

$$y = \frac{f_2(t) * R_1(t)}{f_1(t) * R_2(t) + f_2(t) * R_1(t)}$$
(11)

Plotting eq. (10) and (11) for all failure times will show the region where error will most likely be highest, which occurs near x=y=0.5, meaning that there is a 50% probability that the sorting could be right for either distribution. The plot will also show the region where one distribution has a 100% probability of showing up, with the other distribution having a 0% probability of showing up, meaning that this region can have failure samples sorted to their relative distributions without any inaccuracies. When the distribution's 100% probability lowers, any future time point may have a probability of being sorted incorrectly, which is called the region of error. This region identifies the time periods that are most important for physical failure analysis.

IV. ANALYSIS OF SORTING ERRORS

To determine if there is a difference between the original and MLE extracted parameters, the sorting of samples to their respective failure distributions was performed for both types of parameters. This process was performed by comparing the values of eqs. (2) and (3) at each failure time point to sort the samples. The region of error, found by using eqs. (10) and (11), and the sorting accuracy were also calculated using both types of parameters. The results are summarized below.

A. Sorting Errors Using MLE Extracted Parameters

The sorting for each sample, the calculation of region of error, and accuracy were determined using the MLE extracted parameters. As shown in Fig. 2, there is a region of no error at the smaller failure times due to samples coming from only the dominant wearout mechanism (probability =100%), and this region becomes larger when either the sample size or β ratio is decreased. When the β ratio is about the same, there is no region with no error. The sorting accuracy increases as the β ratio increases, but varies slightly with a difference in sample size. When the percentage of each failure distribution is near 50%, there is a higher probability of the samples being sorted to the wrong distribution, because the risk of the wrong categorization is around 50% too. This information can be used to signal that the samples near this area are the only ones that one may need to perform failure analysis using transmission electron microscopy, not the entire lot, which saves analysis costs. The sorting accuracy is higher than 87.3% for β ratios larger than 4.39 and can reach as high as 100.0%. When the β ratio is about the same, the sorting accuracy is still higher than 70%.

B. Sorting Errors Using Original Weibull Parameters

The same sorting procedure, along with region of error accuracy, were carried out using the original Weibull parameters to compare results with the MLE extracted calculations. In terms of sorting accuracy, region of error, and wrongly sorted failure time, the results were comparable, with similar accuracies. The only difference between using the original and extracted MLE Weibull parameters is in the accuracy of the value of the parameters themselves, as shown in Table IV, but the correct failure mechanism can still be found. In fact, the sorting accuracies are almost the same as with extracted Weibull parameters. Therefore, methodology can be used as a fast way to determine the wearout mechanism for each failure sample.

V. APPLICATION TO TROJAN DETECTION

The methodology of extracting wearout parameters with MLE can also be applied to detect Trojans and to select suspicious samples for failure analysis. Instead of extracting parameters for two confounded distributions, we assume a known distribution for mechanism 1, and use MLE to extract the parameters for mechanism 2 based on the data. Since hardware Trojans are triggered by unlikely events and accelerate a specific wearout mode depending on its design, we consider a worst-case scenario, where the original GTDDB parameters are β_1 =1.64, η_1 =10 yrs, and Trojan affected samples have altered GTDDB parameters to $\beta_2=1.64$, $\eta_2=5$ yrs in a

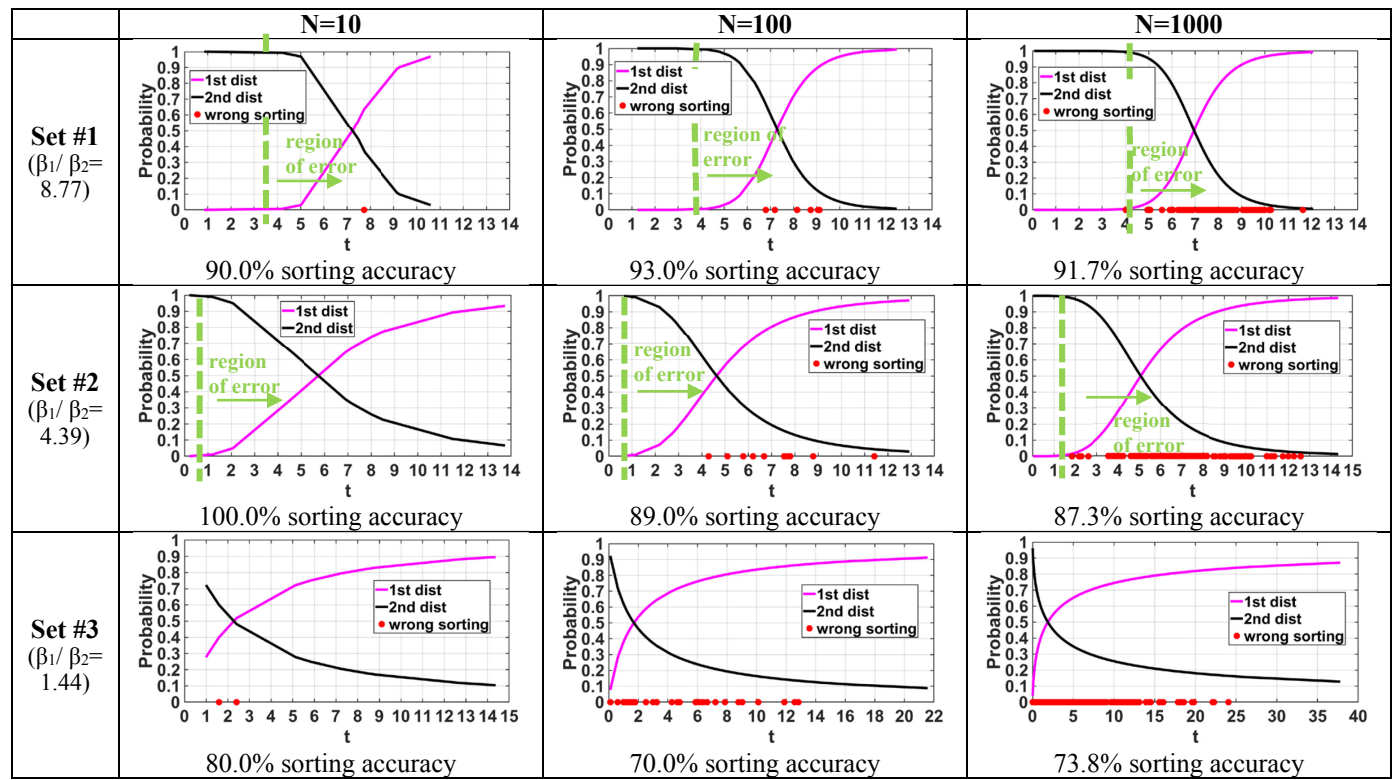


Fig. 2. Percentage of each failure distribution for each failure time point (unit of time: yrs) sorted using MLE extracted parameters, with region of error and sorting accuracy. 1st distribution refers to the 1st wearout mechanism, and 2nd distribution refers to the 2nd wearout mechanism.

TABLE IV SEPARATION ACCURACY FOR MLE EXTRACTED PARMETERS

TTHUMBTERS							
Sample Size	Set #1	Set #2	Set #3				
10	90.0%	100.0%	80.0%				
100	93.0%	89.0%	70.0%				
1000	91.7%	87.3%	73.8%				

14nm FinFET 501-stage ring oscillator. Although the GTDDB β parameters could be different, the hardest case to distinguish is when they are exactly the same, with the only difference being the failure time, where η , also known as the characteristic lifetime, is changed to fail faster. Our algorithms will assign samples to the two distributions and determine the region of error (time points) where samples are likely to be generated by the Trojan. The cause of failure of these samples can then be analyzed.

The comparison of the results for the original GTDDB and Trojan altered samples are shown in Table V. The results demonstrate that MLE can distinguish samples with

accelerated failure lifetime under the same failure mode. which can be used to indicate that Trojan samples exist. Furthermore, the positions of wrongly sorted samples are shown in Fig. 3. Because the β parameters, which determine the failure mode, are the same, only the n parameters, or characteristic lifetimes, affect the sorting accuracy. Since the failure mode is the same, the failure probability will always be higher for the smaller failure time point, η_2 (altered Trojan sample), at each time point, resulting in the parallel lines for the original GTDDB and Troian distributions seen in Fig. 3. This also means that it is easier to have an error when the failure lifetimes are smaller for these special case scenarios, because if an occasional sample belonging to the original GTDDB distribution fails earlier than expected, the sorting will be incorrect. This is also why the sorting accuracy decreases as the sample size increases, because a larger sample size will have a higher probability of sampling original GTDDB samples that fail early. However, the overall sorting accuracy is still higher than 75%, and can be as high as 90%, which indicates that this methodology is still suitable as a

TABLE V COMPARISON OF ORIGINAL GTDDB AND TROJAN ALTERNATED RING OSCILLATORS

Sample	Original GTDDB				Trojan Altered GTDDB				Sorting
Size	β average	error	η average	error	β average	error	η average	error	Accuracy
10	1.377	-16.063%	8.041	-19.594%	1.377	-16.063%	3.206	-35.889%	90.0%
100	1.613	-1.617%	10.305	3.045%	1.733	5.683%	4.962	-0.754%	80.0%
1000	1.603	-2.233%	10.079	0.794%	1.668	1.691%	4.980	-0.405%	77.4%

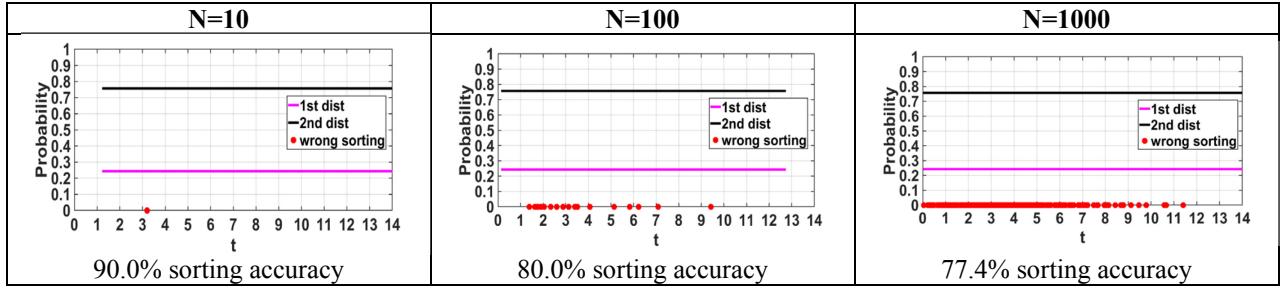


Fig. 3. Percentage of each failure distribution for each failure time point (unit of time: yrs) sorted using MLE extracted parameters, with sorting accuracy. 1st distribution refers to the original GTDDB distribution, and 2nd distribution refers to the Trojan altered distribution.

quick and easy screening process to detect Trojan altered samples.

VI. CONCLUSION

Through maximum likelihood estimation, and probability analysis, we have demonstrated a methodology to determine the wearout mechanism in samples with competing wearout mechanisms. The region of error can be determined for each set of competing wearout mechanisms, and decreases when either the β ratio or sample size is increased. The area where the percentage of each failure distribution is near 50%, meaning that there is a higher risk of wrong sorting, can be used to signal that the samples near this point are the only ones that need physical failure analysis, rather than the entire lot, which can cut down costs.

The sorting accuracy is also more accurate when the β ratio increases but varies slightly with sample size. The results of the sorting process using the MLE extracted and original Weibull parameters are the same. The only distinction may be in the accuracy of the exact values of the Weibull parameters, but this can be minimized with optimized MLE calculations. However, the wearout mechanism can still be determined without any difference with regard to either the extracted MLE or original parameters. The methodology was also applied to detect hardware Trojans, and was able to distinguish the altered samples. Therefore, this procedure provides a quick and non-invasive way to carry out low cost failure analysis and a better way to select samples for costly physical failure analysis.

ACKNOWLEDGMENTS

The authors would like to acknowledge Dr. Yi-Da Wu and Li-Hsiang Lin for their discussions. The authors would like to thank the NSF for support under Award Number 1700914.

REFERENCES

- [1] Y. Shiyanovskii, F. Wolff, A. Rajendran, C. Papachristou, D. Weyer, and W. Clay, "Process reliability based trojans through NBTI and HCI effects," in *NASA/ESA Conf. on Adaptive Hardware and Systems*, 2010, pp. 215-222.
- [2] C. Cook, S. Sadiqbatcha, Z. Sun, and S. X. D. Tan, "Reliability based hardware Trojan design using physics-based electromigration models," *Integration*, vol. 66, pp. 9-15, May 1, 2019.
- [3] R. Karri, J. Rajendran, K. Rosenfeld, and M. Tehranipoor, "Trustworthy Hardware: Identifying and Classifying Hardware Trojans," *Computer*, vol. 43, pp. 39-46, 2010.
- [4] B. Liu, Y. Hua, Z. Dong, P. K. Tan, Y. Zhao, Z. Mo, J. Lam, and Z. Mai, "The Overview of the Impacts of Electron Radiation on Semiconductor

- Failure Analysis by SEM, FIB and TEM," in *IEEE Int. Symp. on the Physical and Failure Analysis of Integrated Circuits (IPFA)*, 2018.
- [5] H. Tan, W. Weng, R. Rai, C. Kang, L. Dumas, I. Brooks, A. Katnani, Z. Zhong, C. Hakala, Y. Lu, J. Fretwall, and T. Johnson, "Advanced industrial S/TEM automation and metrology: Boundary of precision," in *Annual SEMI Advanced Semiconductor Manufacturing Conf. (ASMC)*, 2018, pp. 131-135.
- [6] C. Chen and L. Milor, "Microprocessor Aging Analysis and Reliability Modeling Due to Back-End Wearout Mechanisms," *IEEE Trans. on Very Large Scale Integration (VLSI) Systems*, vol. 23, pp. 2065-2076, 2015.
- [7] T. Liu, C. Chen, and L. Milor, "Comprehensive Reliability-Aware Statistical Timing Analysis Using a Unified Gate-Delay Model for Microprocessors," *IEEE Trans. on Emerging Topics in Computing*, vol. 6, pp. 219-232, 2018.
- [8] K. Yang, T. Liu, R. Zhang, and L. Milor, "A Comprehensive Time-Dependent Dielectric Breakdown Lifetime Simulator for Both Traditional CMOS and FinFET Technology," *IEEE Trans. on Very Large Scale Integration (VLSI) Systems*, vol. 26, pp. 2470-2482, 2018.
- [9] X. Li, J. Qin, and J. B. Bernstein, "Compact Modeling of MOSFET Wearout Mechanisms for Circuit-Reliability Simulation," *IEEE Trans.* on Device and Materials Reliability, vol. 8, pp. 98-121, 2008.
- [10] K. Yang, T. Liu, R. Zhang, and L. Milor, "Circuit-level reliability simulator for front-end-of-line and middle-of-line time-dependent dielectric breakdown in FinFET technology," in *IEEE VLSI Test Symp*. (VTS), 2018.
- [11] W. Ahn, H. Zhang, T. Shen, C. Christiansen, P. Justison, S. Shin, and M. Alam, "A Predictive Model for IC Self-Heating Based on Effective Medium and Image Charge Theories and Its Implications for Interconnect and Transistor Reliability," *IEEE Trans/ on Electron Devices*, vol. 64, pp. 3555-3562, 2017.
- [12] E. Wu, J. Suñé, W. Lai, E. Nowak, J. McKenna, A. Vayshenker, "Interplay of voltage and temperature acceleration of oxide breakdown for ultra-thin gate oxides," *Solid-State Electronics*, vol. 46, pp. 1787-1798, Nov. 1 2002.
- [13] K. Okada, K. Narita, M. Kamei, S. Ohno, Y. Ito, and S. Suzuki, "Generalized model of dielectric breakdown for thick and thin SiO₂ and Si₃N₄ films combining percolation model and constant-ΔE model," in IEEE Int. Reliability Physics Symp. (IRPS), 2017, pp. 5B-2.1-5B-2.5.
- [14] E. Y. Wu, "A new formulation of breakdown model for high-κ/SiO₂ stack dielectrics," in *IEEE Int. Reliability Physics Symp. (IRPS)*, 2013, pp. 5A.4.1-5A.4.7.
- [15] J. Yoo, I. Kang, G. Jung, S. Kim, H. Ahn, W. Choi, J. Jun, D. Jang, I. Baek, and J. Yu, "Analysis of electromigration for Cu pillar bump in flip chip package," in *Electronics Packaging Technology Conf. (EPTC)*, 2010, pp. 129-133.
- [16] T. Ishioka and Y. Nonaka, "Maximum likelihood estimation of Weibull parameters for two independent competing risk," *IEEE Trans. on Reliability*, vol. 40, pp. 71-74, 1991.
- [17] D. B. Kececioglu and W. Wang, "Parameter estimation for mixed-Weibull distribution," in *Proc. Annual Reliability and Maintainability Symp.*, 1998, pp. 247-252.
- [18] S. Hsu, K. Yang, and L. Milor, "Machine Learning for Detection of Competing Wearout Mechanisms", in *IEEE Int. Reliability Physics* Symp. (IRPS), 2019.